ELSEVIER

Journal of Structural Geology 29 (2007) 1843–1854

JOURNAL OF STRUCTURAL GEOLOGY

www.elsevier.com/locate/jsg

Compaction microstructures in quartz grains and quartz cement in deeply buried reservoir sandstones using combined petrography and EBSD analysis

Mai Britt E. Mørk*, Kari Moen

Department of Geology and Mineral Resources Engineering, NTNU, N-7491 Trondheim, Norway

Received 14 July 2006; received in revised form 10 August 2007; accepted 14 August 2007
Available online 19 August 2007

Abstract

Sandstone diagenesis involves porosity loss by mechanical and chemical compaction. In this study we have examined relations of diagenesis and microstructures in quartz grains and quartz cement in sandstones from relatively deep burial depths offshore mid Norway. Electron backscatter diffraction analysis (EBSD) has been combined with optical and cathodoluminescence petrography study of samples with different degrees of compaction and quartz cementation. Quartz cement is shown to be syntaxial to the nearest host domain (grain or subgrain), both for monogranular, polygranular, undeformed and deformed quartz. The quartz cement growth may have been initiated at different subgrain surfaces, and preserving pre-depositional deformation structures. EBSD inverse pole figure imaging shows dauphiné twins to be common in all samples, both in quartz grains and quartz cement. The dauphiné twins appear in grain-grain contacts and in cement-crystal boundaries, and commonly crossing grain−cement boundaries. On basis of twin distributions we suggest that both inherited twins from the source area and twins formed by compaction-induced grain boundary deformation are present. A general problem in sedimentary rocks is to distinguish inherited from sedimentary compaction-induced intra-grain deformation structures. This study shows that the role of ductile deformation mechanisms (e.g. twinning) in sediment compaction can be clarified by more comprehensive following up studies using EBSD analysis in combination with other techniques.

Keywords: Sandstone; Compaction; Quartz cement; Dauphiné twins; Electron backscatter diffraction analysis

1. Introduction

Compaction is a reduction in volume due to overburden stress, and sedimentary rocks undergo compaction and porosity reduction during burial and diagenesis. The processes of sediment compaction are commonly divided broadly into mechanical compaction at relatively shallow depth (e.g. <2.5 km depth) and chemical compaction at deeper burial. Mechanical compaction involves grain rotation and breaking, and squeezing of ductile grains all of which contribute to denser packing and reduction in porosity (e.g. Boggs, 1992; Chester et al., 2004). Chemical compaction involves dissolution, element transport and cementation. However, the spatial two-division is broad and over-simplified, as the actual processes are dependent on combinations of several geological parameters. The rate and degree of sandstone compaction is influenced by burial rate, sediment composition, rock- mechanical and petrophysical properties, as well as temperature, pressure and stress conditions. In reality, compaction may be caused by both mechanical and chemical processes in shallow and deeper burial regimes.

In the deeply buried siliciclastic sedimentary rocks, quartz cementation is one of the most important porosity reducing factors (e.g. Bjørlykke et al., 1986; McBride, 1989; Worden and Burley, 2003). Various sources of silica for quartz cement formation have been documented and discussed in the

* Corresponding author. Tel.: +47 73 59 48 12; fax: +47 73 59 48 14.
E-mail address: mai.britt.mork@ntnu.no (Mai Britt E. Mørk).

0191-8141/$ - see front matter
doi:10.1016/j.jsg.2007.08.004

literature (e.g. Boggs, 1992; Aplin et al., 1993; Vagle et al., 1994). Especially mechanisms involved in pressure dissolution at stylolites, i.e. dissolution of detrital quartz and precipitation of authigenic quartz cement, have been reviewed and discussed (Renard et al., 2000). These processes are mainly temperature dependent (Walderhaug, 1996; Lander and Walderhaug, 1999), and the quartz dissolution process is enhanced at sites where quartz grains are in contact with mica or clay minerals (Thomson, 1959; Bjørkum, 1996; Oelkers et al., 1996; Renard and Ortoleva, 1997; Walderhaug and Bjørkum, 2003). In recent models of quartz cementation, stress is considered insignificant in promoting dissolution at grain contacts (Bjørkum, 1996; Renard et al., 2000). However, the role of stress induced grain deformation could be difficult to document in deep burial diagenesis due to grain dissolution and cementation processes.

Cathodoluminescence imaging has a potential to identify deformation structures such as cemented microfractures in quartz (Milliken and Lauback, 2000). In a study of the Frio Formation sandstones in the Gulf of Mexico, Makowitz and Milliken (2003) documented that micro-fracturing in quartz had taken place before, during and after quartz cementation. Fisher et al. (1999) attributed mechanical compaction structures of sandstone at deep (>4.5 km) burial to situations where the rate of stress increase had been higher than the rate of ‘‘chemical compaction processes’’.

In this study, we examine if new combinations of petrographic methods can provide information of micro-structures in quartz grains and quartz overgrowths that can be related to diagenetic compaction. We combine conventional optical petrography and cathodoluminescence analysis with electron backscatter diffraction (EBSD) analysis. We postulate that this type of approach may have a potential to increase our knowledge of deformation and compaction processes in burial diagenesis. The EBSD technique (Schmidt and Olesen, 1989; Prior et al., 1999; Schwartz et al., 2000) has proven successful in fabric analysis in structural geology (e.g. van Daalen et al., 1999; Lloyd, 2000), in prediction of seismic properties (Valcke et al., 2006), and in study of mineral growth mechanisms in igneous and metamorphic petrology (Piazolo et al., 2005; Terry and Heidelbach, 2006). Haddad et al. (2006) recently used the EBSD technique to identify different growth zones in quartz cement that formed during relatively shallow burial conditions. In contrast, we present data from quartz-cemented sandstone of relatively deep burial depth, representative for common sandstone reservoirs offshore Norway, to examine possible microstructures in relation to burial compaction and cementation. The selected sandstones are from exploration wells in central areas of the Halten Terrace (Fig. 1), in the main petroleum exploration area in the Norwegian Sea. The aim is to establish indicators for interpreting compaction and deformation mechanisms in quartz-rich sandstones.

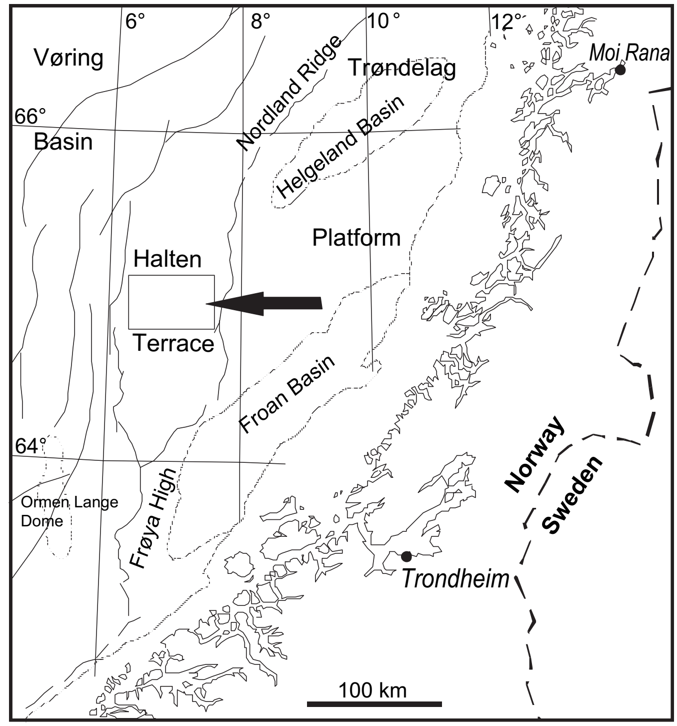

Fig. 1. Location of the Halten Terrace (‘‘Haltenbanken petroleum province’’) in the Norwegian Sea offshore mid Norway. The study area is indicated by a rectangle. Names offshore refer to main structural elements (see Blystad et al., 1995).

2. Analytical procedure

Polished thin sections were examined by optical microscopy for petrographic sandstone characterisation, diagenetic interpretation and selection of samples for further study. Areas of EBSD analysis were selected and identified by SEM backscatter electron images and cathodoluminescence.

The EBSD technique is based on the weak diffraction pattern that forms when a focused, stationary, primary electron beam is located at a specific point on a highly tilted sample (Hjelen et al., 1993; Schwartz et al., 2000; Goldstein et al., 2003). The resulting pattern provides information on the crystal structure and space orientation within the diffracting volume of the electron beam, and the software rapidly reads the pattern and calculates the crystallographic orientation with respect to a given reference system (Wright, 2005). The interaction volume is dependent on acceleration voltage and atomic number of the analysed minerals, and is usually in the submicron range (Pettersen et al., 1998; Humphreys, 2001). To be able to get a pattern that can be indexed, the crystal lattice at the sample surface has to be undeformed. To obtain this, a post-mechanical preparation is required (Lloyd, 1987). After mechanical polishing, the surface damage in the uppermost layers was therefore removed by chemical-mechanical polishing (Prior et al., 1999; Moen et al., 2003). To get optimal EBSD patterns, the analyses were performed using a low vacuum SEM (Hitachi S-3500N), and without a conductive carbon layer. The equipment applied for the experiments includes a Nordif EBSD digital camera, and using the TSL, OIM (orientation image microscopy) software. The following running and processing conditions for EBSD mapping were applied: working distance 20 mm, 20 kV accelerating voltage, <30 Pa pressure, 70° tilt, and 2 × 2 binning (CCD camera readout pattern). Identical working distance, accelerating voltage and pressure were used during CL analysis.

3. Geological framework

The early Mesozoic deposition and subsidence history in the Norwegian Sea—Haltenbanken area is related to tectonic rifting, followed by Cretaceous and Tertiary post-rift subsidence, and then pronounced Neogene subsidence (Spencer et al., 1993). A stratigraphic overview of the Mesozoic sedimentary rocks is given in Dalland et al. (1988). The studied samples are from sandstones of the Lower Jurassic Åre and Tofte formations, and from the Lysing Formation (Cromer Knoll Group) of Late Cretaceous age. The depositional environments are interpreted as respectively fluvial–paralic in the older formations and fully marine in the younger (e.g. Dalland et al., 1988; Shanmugam et al., 1994; Brekke et al., 2001). Both eastern and western areas of the Caledonides may be source areas for the Jurassic sands (Gjelberg et al., 1987; Brekke et al., 2001), and western and northern marginal areas, including Greenland, for the Cretaceous formations (Morton and Grant, 1998; Brekke et al., 2001). Deeper parts of the orogen comprising metamorphic schists, gneisses, and granites were exposed for erosion already in early Mesozoic time (Mørk and Johnsen, 2005). The regional geothermal gradient has been fairly high through time, possibly as high as 35 °C/km (Oelkers et al., 1996). The present formation depths at the Halten Terrace are close to the maximum burial depths (Spencer et al., 1993), and the most prominent subsidence with burial from 3 to 5 km for the Jurassic formations took place during the last 10 Ma (e.g. Karlsen et al., 2004). Diagenesis and quartz cementation of Jurassic reservoir sandstones from the Halten Terrace are discussed by Bjørlykke et al. (1986, 1989); Ehrenberg (1990) and Storvoll et al. (2002). Extensive quartz cementation in the sandstones has been documented from 3.5–4.5 km and greater burial depths and the cementation took place relatively late in the burial history (Bjørlykke et al., 1989). Based on fluid inclusion studies Walderhaug (1994) interpreted the main quartz cementation to have taken place at temperatures of 80–120 °C. Findings of intervals of unusual high porosity values in the deepest buried sandstones are ascribed to inhibition of quartz cementation by presence of grain-coating chlorite or illite/chlorite (Ehrenberg, 1993; Storvoll et al., 2002).

Samples for the present study were selected from cores in different exploration wells to cover cases of different diagenetic compaction/cementation relations. Using an average regional geotherm of 30 °C/km, the studied sandstones from 3.2 to 5 km burial depths experienced maximum temperatures of ~100–150 °C, whereas maximum values of 115–175 °C are obtained using the mentioned value of 35 °C/km (Oelkers et al., 1996).

4. Sandstone petrography and diagenesis

Three categories of sandstones are described below; sandstones with extensive quartz cementation (category A, Fig. 2a and 3), deeply buried sandstone with very little quartz cementation (category B, Fig. 2c and 4) and a stylolite-bearing sandstone with minor clay matrix and clay laminae (category C, Fig. 5a). Mineralogical compositions are quantified by petrographic modal analyses using 600 counts (Table 1a). The compositions are relatively quartz-rich, classifying as subarkosic arenite (Pettijohn et al., 1972). The main diagenetic features as interpreted from optical petrography are summarised below. Diagenetic quartz overgrowths on quartz grains have been identified by location of dust/inclusion rinds, and by grain shapes and textural relations. Further, such overgrowths have been confirmed by dark coloured rims in cathodoluminescence images (Fig. 2a,b and 3) (e.g. Sippel, 1968; Oelkers et al., 1995).

Compaction can be interpreted from petrographic modal analysis. As both compaction and cementation have taken place in the studied sandstones, porosity reduction alone does not give a correct value for the amount of compaction. In such cases, changes in intergranular volume (IGV) as defined by the sum of porosity and pore-filling cements (Beard and Weyl, 1973; Paxton et al., 2002) give better indications of compaction. Uncertainties in calculating IGV relate to interpretation of dissolution porosity and replacive cements which are subtracted from the IGV values (Table 1b).

4.1. Category A. Quartz-cemented samples

Sample 3185 (Lysing Formation) is from a medium to coarse-grained, moderate-well sorted sandstone with 24% quartz cement (Fig. 3a) and 14% porosity. The presence of glauconite suggests eogenesis in a marine environment prior to the burial diagenesis. The main phase of quartz cementation is predated by pore-filling kaolinite. The latest diagenetic event involved precipitation of coarse carbonate cement (sporadically distributed) and dissolution of detrital feldspar. The calculated IGV value of 41% is close to primary porosity values in arenitic sandstones, in spite of burial depths >3 km. This suggests that the quartz cementation in this sandstone was relatively early in the diagenetic history, and that it prevented extensive compaction in this interval.

Sample 4205 (Tofte Formation) is medium to very coarse-grained, poor to moderately sorted with 19% quartz cement (Fig. 2a) and 7% porosity. Minor clay-mineral coatings around quartz are interpreted as early diagenetic and appear to predate dissolution of detrital feldspar grains. Authigenic kaolinite, pyrite and siderite predate the main phase of mesogenetic quartz cementation. The quartz cement growth was postdated by dissolution of detrital feldspar and by growth of carbonate cement, which occurs in minor amounts only. The calculated IGV value of 28% suggests a larger degree of compaction than in case 3185 for this deeper buried sandstone.

4.2. Category B. Samples with limited quartz cement

Sample 5040 (Åre Formation) is from a medium to coarse-grained, well-sorted arenitic sandstone with 9% porosity and only 2% quartz cement. This sample has relatively dense grain

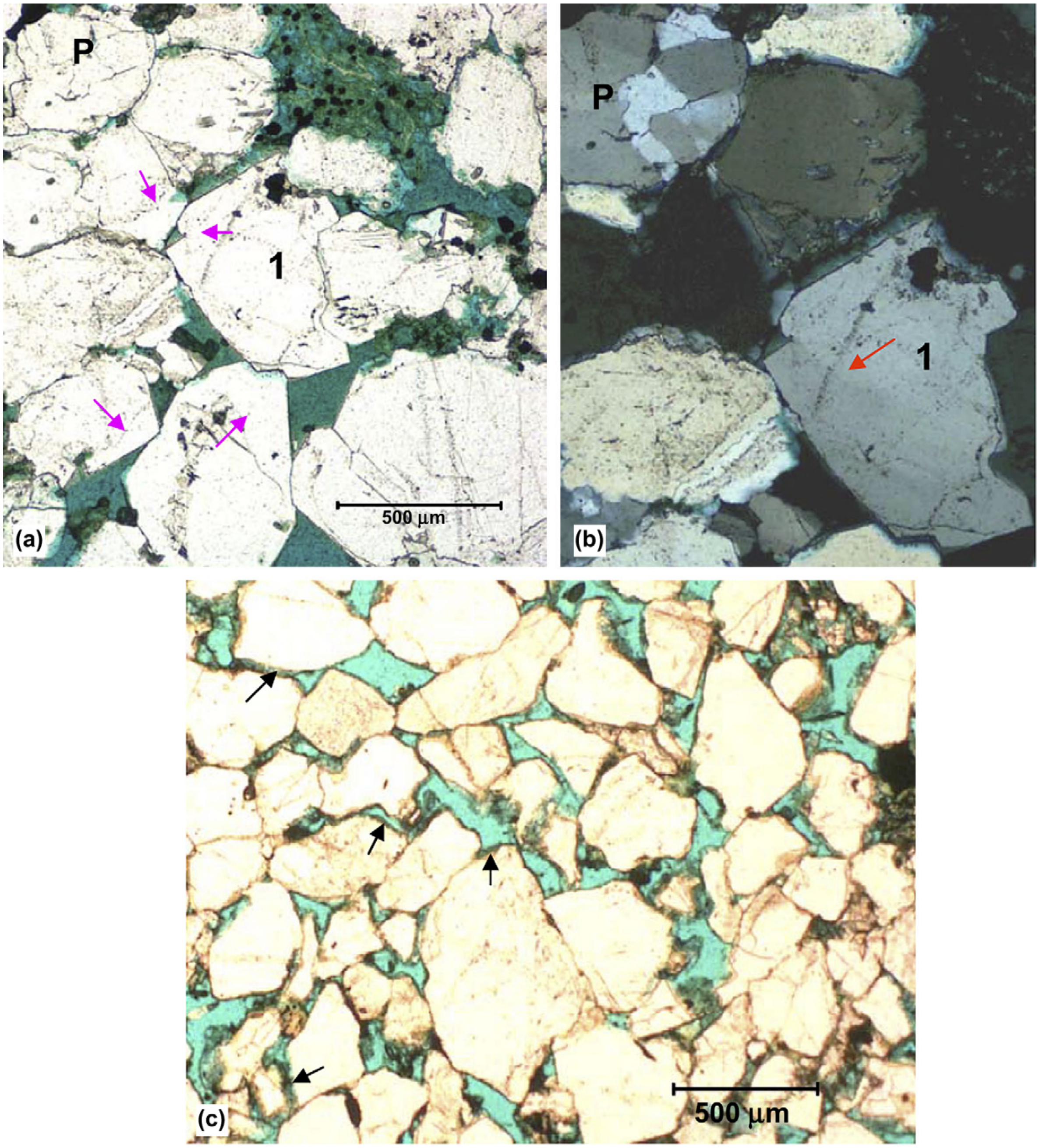

Fig. 2. Optical micrographs of sandstones. Porosity is shown by blue colour. (a) Sandstone category A, sample 4205 (plane polarised light), shows porosity loss due to quartz cementation (see arrows). (b) Close up of (a) in crossed polarised light show examples of quartz overgrowths on detrital grains that include subgrains (low angle boundaries) (arrow in grain 1) and on polygranular grains (P). (c) Sandstone category B, sample 5040, showing reduced porosity due to packing of the detrital grains (plane polarised light). Dark rims include grain coating chlorite (see arrows).

packing (Fig. 2c). The detrital quartz and feldspar grains have thin clay-mineral coatings. Similar clay-mineral coatings also preserve the outline of partly dissolved feldspar grains. Carbonate cement has precipitated into partly dissolved feldspar grains, and late carbonate cementation is supported also by presence of compacted and folded mica flakes included in the carbonate cement. Siderite and pyrite form aggregates in local domains. The absence of quartz cement may be due to the chlorite coatings which cover the detrital quartz surfaces, reducing optimal sites for diagenetic quartz overgrowths (cf. Ehrenberg, 1993; Storvoll et al., 2002). The calculated IGV values of 18% imply considerable compaction, both mechanical and chemical. The late stages of mechanical compaction (squeezing of grains) may have been facilitated by feldspar dissolution.

4.3. Category C. Sample with stylolite lamina

Sample 5243 (Åre Formation) is from a medium to very coarse-grained, poorly sorted, sandstone with clay laminae

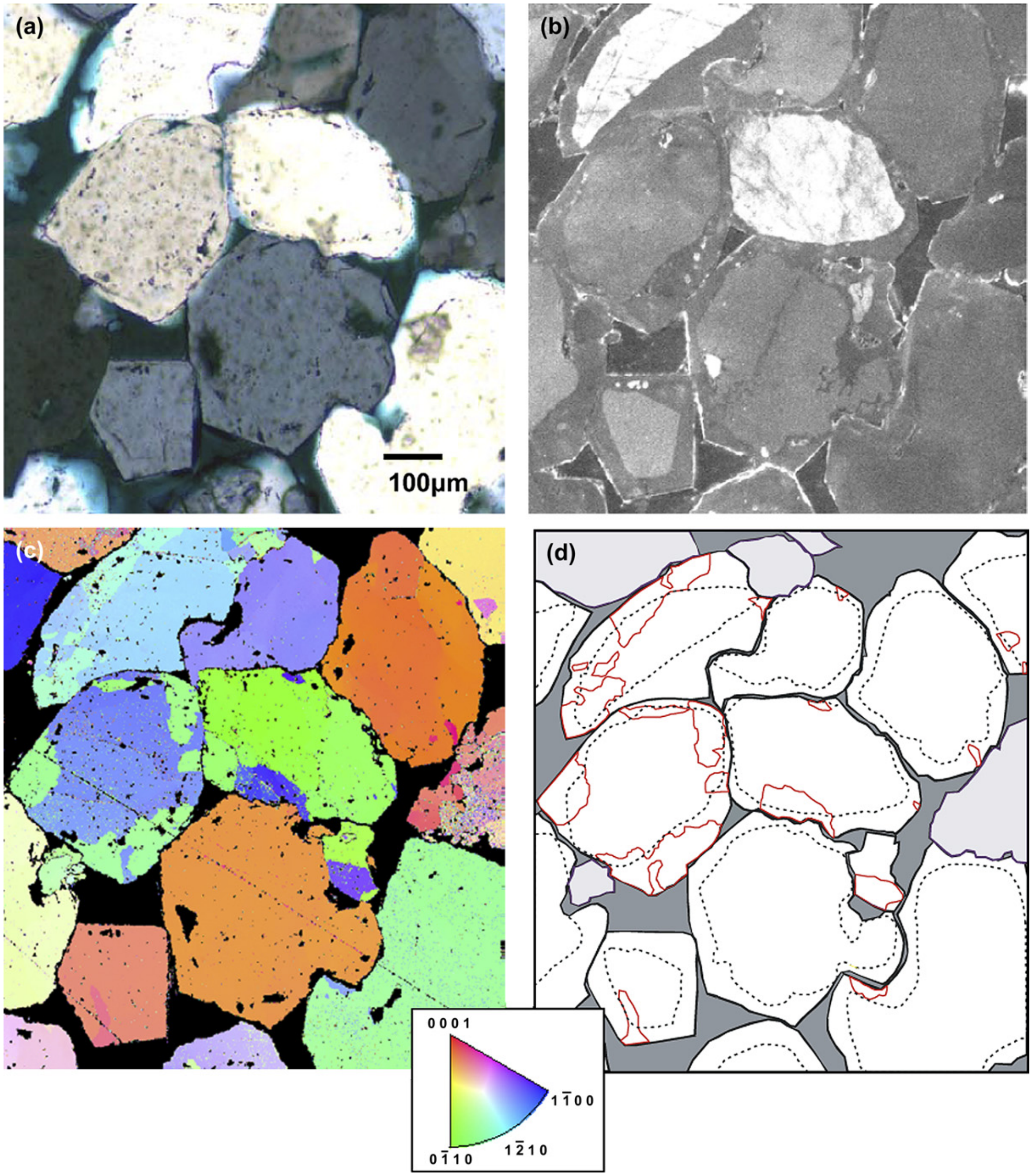

Fig. 3. Microstructural relations of quartz cement overgrowths and dauphiné twins in sample 3185. (a) Optical micrograph (crossed polars). (b) Cathodoluminescence image showing the overgrowths as dark rims on the quartz grains. (c) EBSD orientation image of quartz, step size 1 μm. Crystal orientation normal to the image plane is shown by colour code in the small inset figure. (d) Composite sketch showing quartz with overgrowths in white, with original detrital grain boundaries shown by dotted line. Dauphiné twins are shown with red boundary lines.

and with 5% porosity and only minor (2%) quartz cement. Stylolites are developed at the thin clay lamina (Fig. 5a). The stylolite formation and mica compaction is post-dated by feldspar dissolution and late carbonate cement. The low porosity reflects a combination of clay matrix, mechanical compaction and late carbonate cement. As the amount of original matrix is uncertain, the IGV of 16% can not be used to establish the degree of compaction. However, assuming dissolution at stylolites, compaction could have been considerable.

4.4. Summary of compaction

In summary, sandstones from categories B and C show evidence of significant compaction, reflecting a combination of mechanical and chemical compaction. These samples show more compaction than the limit for mechanical sandstone compaction that is defined on basis of total IGV values (IGV = 26%) (Paxton et al., 2002). To the contrary, the large IGV values in category A sandstones show that quartz

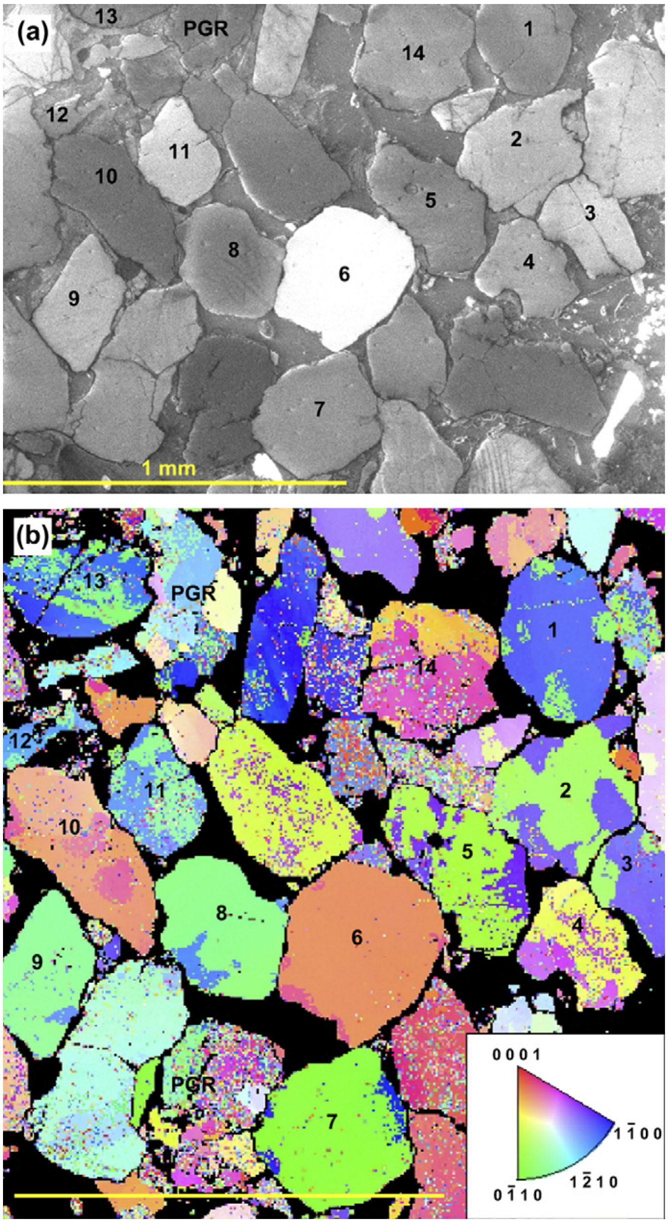

Fig. 4. Cathodoluminescence image (a) and EBSD inverse pole figure map (b) of relatively densely packed sandstone (sample 5040). Grains with distinct dauphiné twins are numbered. Note patchy dauphiné twin distributions. The smallest, pixel sized spots are considered to be noise due to mis-indexing. Step size: 5 μm. PGR, polygranular grains. Inset as in Fig. 3.

cementation may have occurred relatively early in mesogenesis at these sites, and was more important than compaction in reducing porosity.

5. Microstructures of quartz grains and quartz cement

The detrital mineral grains in sedimentary rocks are derived by erosion from a variety of metamorphic, igneous or sedimentary source rocks which have experienced different temperature, pressure, deformation and exhumation histories in the past. This means that there may be slight variations in the deformation state of the detrital quartz grains in the sandstones prior to burial and compaction. Deformation mechanisms of rocks in general are categorised into diffusive mass transfer (DMT), crystal plasticity, frictional sliding, fracture processes and cataclastic flow (e.g. Knipe, 1989). Diagenetic processes involve mostly inter-grain processes, (mechanical deformation and diffusive mass transfer mechanisms). Intracrystalline processes such as dislocation creep and twinning (e.g. Barber, 1985; Groshong, 1988; Knipe, 1989) are facilitated at higher temperatures. As the quartz cement has experienced only diagenetic temperatures (<100–175 °C), it is of particular interest to compare microstructures of the detrital quartz grains and the diagenetic quartz cement.

The detrital quartz in all the studied sandstone categories can be divided into either monogranular (90–75%) or polygranular (10–25%) grains. The latter include slightly foliated aggregates which may have originated from metamorphic rocks and some coarser-grained aggregates in which the quartz is identical to the monogranular quartz. Quartz cement occurs as syntaxial overgrowths on both mono- and polycrystalline quartz grains. Where quartz overgrowths are present on polygranular grains the overgrowths show similar crystallographic orientation as the various crystals they overgrow, giving slight variations in crystal orientation within an overgrowth zone. This is seen under the optical microscope (e.g. Fig. 2b and 6e), and confirmed by EBSD analyses.

The EBSD analysis was performed to obtain information about deformation microstructures in quartz grains and quartz cement. EBSD data are represented as crystal orientation maps prepared from inverse pole figures (Fig. 3c, 4b, 5b and 6c). The colour code refers to crystallographic orientation vertical to the sample (image) plane. The EBSD images are compared with optical microscope images and SEM backscattered electron images as well as cathodoluminescence images. The data are also presented in special grain boundary maps that verify distributions of high angle boundaries, low angle boundaries and 60° twin boundaries (e.g. Fig. 6b,d). The quartz grains within the small sample areas that were studied apparently show random orientations.

5.1. Low angle boundaries and cement

A high proportion of the monogranular quartz grains show distinct low angle boundaries in all the studied samples, as identified by both optical and EBSD analyses. Subgrains are defined by maximum misorientations of 10° (White, 1977; Vernon, 2004). These boundaries can be interpreted as "walls" of organised dislocations formed by strain redistribution (recovery) by dislocation creep in the crystals (Vernon, 2004).

Where quartz overgrowths are present on grains with subgrains defined by low angle boundaries, the overgrowths show similar crystallographic orientation as the different subgrains (Fig. 2b and 6e). This is confirmed by EBSD analyses (Fig. 6d). The observation of low angle boundaries both in detrital quartz grains and in the quartz cement is unexpected as low angle boundaries are associated with deformation under metamorphic conditions (e.g. Vernon, 2004). The above

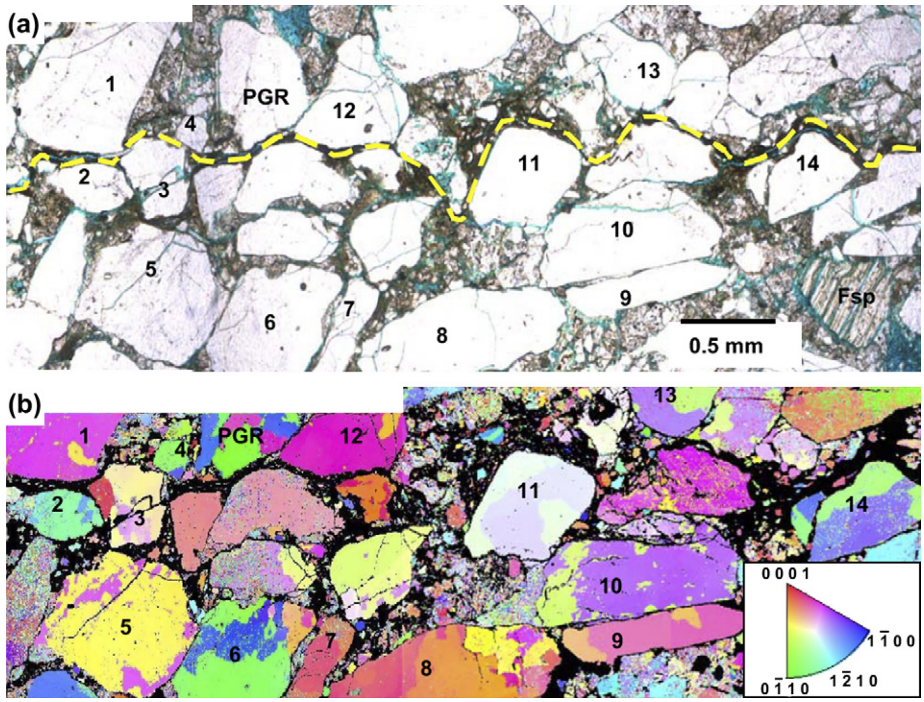

Fig. 5. (a) Optical images (plane polars) of sandstone sample 5243. The yellow line locates a micro-stylolite. The quartz grains (white) are surrounded by clay matrix and carbonate cement (brown), and minor porosity (blue). Note partly dissolved feldspar (Fsp, lower right side). Numbers refer to grains with distinct dauphiné twins in (b). PGR, polygranular quartz. (b) EBSD image showing examples of patchy dauphiné twins in grains 1–14. Step size: 5 μm. Inset as in Fig. 3.

observations suggest either cement growth preserving the small variations in orientations of the detrital host lattice, or alternatively, deformation during the burial. The second alternative, that subgrain boundaries formed in response to deformation after cement growth is less likely, as the mechanisms of subgrain formation are more effective at higher temperature conditions (e.g. Groshong, 1988; Vernon, 2004; Passchier and Trouw, 2005).

5.2. Dauphiné twinning

Dauphiné twins are related by a 180° (or apparent 60°) rotation about the quartz c(0001) axis. Such twins are not visible by optical microscopy, but can be identified by the electron backscatter diffraction techniques (Schmidt and Olesen, 1989). Dauphiné twinning is commonly seen to emanate from a region of contact with a neighbouring grain. Several processes can cause dauphiné twinning: structural inversion from β- to α-quartz during cooling (Putnis, 1992; Nord, 1994), grain boundary migration due to contact metamorphic heating (Piazolo et al., 2005), and stress (e.g. Frondel, 1962; Tullis, 1970; Lloyd, 2000; Wenk et al., 2005). Lloyd (2000) interpreted dauphiné twins at quartz grain contacts as penetration twins caused by stress concentrations related to faulting.

5.2.1. Category A. Quartz cemented sandstones

Sample 3185: Dauphiné twins occur as small patches at long contacts and at quartz cement edges, in some cases cross-cutting cement–grain boundaries. Twins are also developed in overgrowths in contact with pyrite which predates the quartz cement. Fig. 3c,d show dauphiné twins restricted to cement rims as well as dauphiné twins that include both cement and outer parts of host grains.

Sample 4205 shows similar features as described above for sample 3185. The dauphiné twins are located at long grain boundaries, in quartz-cemented zones and in contact with other grains or cement zones. The twin boundaries appear to

Table 1a
Modal analysis (%) of sandstones selected for EBSD study

Category	Sample	Qtz	Qtz pgr	Fsp	Mic	Rfr	Cly lam	Aut. cly	Carb cem	Opq cem	Qtz cem	Por	Total IGV
A	3185	47	0	5	<1	4	0	5	<1	0	24	16	41
A	4205	48	12	6	1	0	0	4	1	2	19	7	28
B	5040	59	7	7	2	1	0	6	7	2	2	9	18
C	5243	51	8	10	<1	0	4	5	14	<1	2	5	16

IGV refers to inter-granular volume, excluding replacive cement (Table 1b). Mineral abbreviations: Qtz, quartz; Qtz pgr, polygranular quartz; Fsp, feldspar; Mic, mica; Rfr, rock fragment; Cly lam, clay laminae; Aut cly, authigenic clay minerals; Carb cem, carbonate cement; Opq cem, opaque cement, pyrite; Qtz cem, quartz cement; Por, porosity.

Table 1b
Supplementary data from modal analysis

Analysis	Replacive cement	Porefill cement	Porosity secondary	Porosity primary	IGV
3185	3	25	<1	16	41
4205	4	22	2	6	28
5040	7	10	1	8	18
5243	7	14	3	2	16

crosscut both fluid-inclusion trails that mark the "pre-cement" grain boundary, and zones at grain edges.

5.2.2. Category B. Sandstone with limited quartz cement

Sample 5040: This sandstone shows examples of patchy dauphiné-twin localisation at detrital grain edges near the contact with other quartz grains (Fig. 4b, e.g. grains marked 1 and 7). Twins are also developed adjacent to patchy carbonate cement or clay mineral and carbonate rims. Such twin distributions at grain boundaries may suggest a relation to post-depositional compaction deformation. However, dauphiné twins in quartz also occur near to pores (Fig. 4b), but it is possible that other grains may be in contact when considering the 3D space. It is also possible that adjacent grains may have been dissolved during a later event.

5.2.3. Category C. Sandstone with stylolite lamina

Sample 5243: Quartz grains are elongated and share long contacts subparallel to the stylolite seam and at a steep, oblique angle. The EBSD image (Fig. 5b) indicates a random orientation of quartz grains along the stylolite. Patchy dauphiné-twin bodies occur on one or both sides of high angle, long grain contacts (e.g. grain 5, Fig. 5b), and occasionally at grain edges (grain 9). Other grains show dauphiné twins that may be inherited.

5.2.4. Relation to subgrains

Dauphiné twins are seen to occur in quartz grains with or without subgrains, which are believed to be inherited structures. In some instances they are located only in parts of subgrains, but they are also seen to cross subgrain boundaries (Fig. 6).

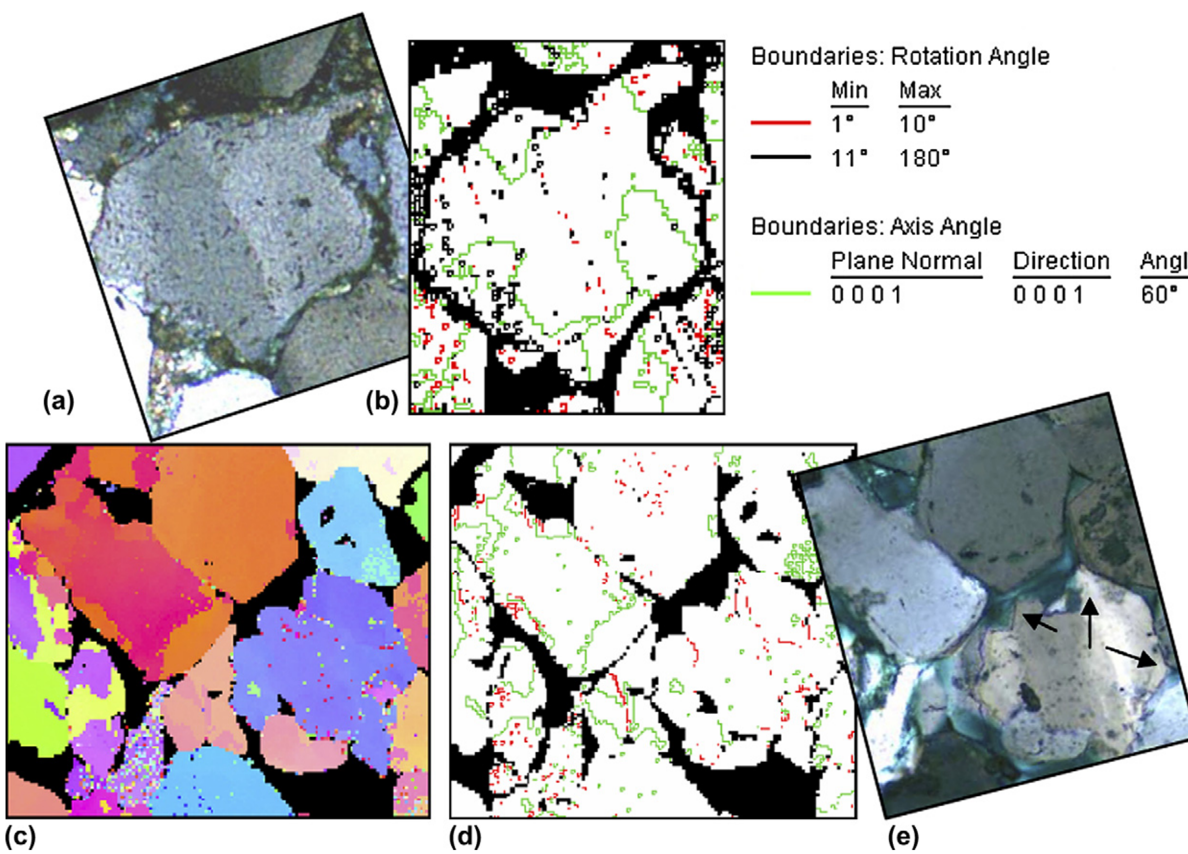

Fig. 6. Examples of low angle (subgrain) boundaries and dauphiné twins in quartz shown by red and green lines, respectively. (a) Optical micrograph (crossed polars), sample 5040 showing low angle boundaries in detrital quartz. Compare with (b) grain boundary map showing both dauphiné twin boundaries and low angle boundaries (red colour) and EBSD image Fig. 4 (grain 2). Step size: 5 μm. The smallest, one-pixel sized spots are considered to be noise due to mis-indexing. (c–e) Sample 3185. Detrital quartz grains with diagenetic quartz overgrowths are shown. The overgrowths can be recognised in the optical micrograph (crossed polars) (e). (c) EBSD image and (d) grain boundary map showing dauphiné twins and low angle (subgrain) boundaries. The twin and low angle boundaries continue into the quartz overgrowths (arrows in e).

6. Discussion

In interpreting deformation from natural rocks there are numerous uncertain parameters like fluid history, burial rate, thermal history, and only parts of the history can be interpreted from the preserved microstructural relations. The sandstones in the present study experienced burial and diagenesis through the passage from surface conditions to maximum burial depths of 3–5 km under relatively high geothermal gradients. The original sandstone porosity has been reduced by a combination of different diagenetic processes. Quartz cementation was the main porosity reducing factor in the category A sandstones, and mechanical compaction in category B and C sandstones. The main compaction and quartz cementation was followed by late diagenetic carbonate cementation in all cases. In the category B sandstone from relatively deep burial, quartz cementation was prevented due to the presence of clay mineral coatings on the detrital grains. Partial dissolution of feldspar could have facilitated increased mechanical compaction in the later part of the burial history. The matrix bearing, stylolite bearing sandstone (category C) experienced compaction by a combination of mechanical grain rotation and dissolution at the stylolite before late precipitation of carbonate cement. In total, the selected sandstones provide different scenarios for studying relations between compaction and cementation.

The interpretation of relatively early mesogenetic quartz cementation in the younger of the category A sandstones (Cretaceous, Lysing Formation) differs from the well established models of late burial diagenetic quartz cementation of Jurassic sandstones at the Halten Terrace (e.g. Bjørlykke et al., 1986; Ehrenberg, 1990). Gluyas et al. (1993) attributed extensive quartz cementation to thermal episodes related to changes in burial rates and fluid migration history. Such episodes could explain the quartz cementation of the younger category A sandstones. Anomalous porosity-depth and quartz cementation trends are also described from deep marine Cretaceous sandstones in adjacent areas (Lien et al., 2006).

The EBSD data show the frequent occurrence of dauphiné twins in quartz grains in all the three categories of sandstones, and also in the diagenetic quartz cement in the category A sandstones. The dauphiné twins could in principle have different origins: (1) inherited from the metamorphic source area, i.e. formed prior to erosion and deposition, (2) formed after deposition by deformation at grain boundaries prior to quartz cement precipitation, and (3) by deformation during or following quartz cementation. The twin patches show different distributions and size, and we suggest that some of the larger ones located within or across grains could be inherited twins from the metamorphic or igneous source rock histories. The relation of dauphiné twins to quartz overgrowths was examined by combining EBSD images with optical microscopy and cathodoluminescence images (Figs. 3 and 6). Patchy dauphiné twins are seen to crosscut the original quartz grain–quartz overgrowth boundaries. Occasionally they appear only in the quartz overgrowth, in some grains they occur at cement–cement contacts between different grains, in cement in contact with early formed pyrite, but also in cement near to pores (e.g. samples 3185 and 4205). These relations give evidence of twin formation at diagenetic conditions, either during and/or after the quartz cement growth. However, the detailed mechanisms remain questionable, since they either formed as growth twins controlled by the orientations of older twins in the detrital grains, or by compaction induced deformation during or after cement precipitation. A third alternative such as twin boundary migration recrystallisation is known from more elevated temperatures (e.g. in calcite, Vernon, 1981) and is probably not a likely mechanism in this case of diagenesis. A possible interpretation is that the smaller twin patches aligned in the cement and around grain–cement boundaries are due to diagenetic compaction, whereas larger patches, dominantly within the detrital grains are inherited twins.

In the compacted sandstone without quartz cement, the apparent spatial relationship of patchy dauphiné twins to the present sedimentary grain contacts suggests that the twins have formed in response to compaction induced stresses. This interpretation is supported by the documentation of stress induced dauphiné contact twins in other studies (Frondel, 1962; Hartley and Wilshaw, 1973; Lloyd, 2000; Wenk et al., 2005, 2006). Experimental results by Laughner et al. (1979), showing that dauphiné twins could be formed in quartz at stresses down to 0.9 kb, is particularly relevant to the present study.

Assuming that the dauphiné twins formed due to burial diagenetic compaction, why are they developed at some contacts, and not all? To answer this question, several factors including grain orientation, stress distributions and diagenetic history must be considered. Influences of grain orientation relative to the principle stress axes is shown in a recent detailed experimental study of cryptocrystalline quartz (novaculite) (e.g. Wenk et al., 2006), documenting most successful twin formation for grains oriented with the $02\bar{2}1$ pole parallel to σ_1. In the Mesozoic sandstones in the present study, the quartz shows no preferred orientation within the limited data sets, and twins are seen to occur for the different quartz grain orientations. Another factor is that even in the most simplified model of simple spheres, experimental deformation and mathematical stress simulations have shown the distribution of grain contact stress to be heterogeneous, with largest stress magnitudes in trains at relatively small angles to σ_1 (e.g. Gallagher et al., 1974; Fjær et al., in press). Natural sandstones as exemplified by the Mesozoic sandstones in the present study show complex textural relations and heterogeneities with respect to grain sizes and mineral properties, and the grain contact stress magnitudes would depend on whether the grains are load-bearing or not (e.g. Giles et al., 2000). Finally, diagenesis results in changes in grain configurations and grain contact stress distributions through time. Cementation would result in more uniform stress distributions and reduce the stress at each grain contact (Gallagher et al., 1974), as would also presence of longer grain–grain contacts which could result from diagenetic dissolution. Selective mineral dissolution (e.g. feldspar) could also locally lead to readjustment of the adjacent quartz–grain configuration during further compaction. In summary, even if conditions are appropriate for formation of grain contact twins in different stages of the burial history, the spatial distribution of contact twins is likely to be heterogeneous.

Twin formation and fracturing are different responses to applied grain boundary stress in quartz (Hartley and Wilshaw, 1973). The intra-grain deformation structures most commonly described in literature on sandstone diagenesis and compaction (e.g. Fisher et al., 1999; Makowitz and Milliken, 2003) and confirmed by experimental work (e.g. Schutjens, 1991; Chester et al., 2004) involve microfractures. However, mesogenetic processes tend to obliterate the early deformation structures as strained grains would be more soluble than unstrained ones, and fractures would be annealed by cementation. Parts of the deformation history can be interpreted from identification of cemented microfractures, e.g. by cathodoluminescence microscopy (Milliken and Lauback, 2000; Makowitz and Milliken, 2003). With basis in the present study we suggest that EBSD analysis in combination with other methods has a potential in the study of sandstone diagenesis and compaction for interpreting stress distributions and relations between grain deformation and quartz cementation. A quantitative study using samples that are oriented relative to paleo-strain indicators is suggested.

7. Conclusions

EBSD in combination with optical microscopy and cathodoluminescence analysis of sandstones verified that diagenetic quartz overgrowths are syntaxial to the detrital quartz grains. In polygranular quartz aggregates the overgrowths are syntaxial to the orientation of the nearest host crystal in the aggregate. Similarly, subgrain boundaries of the detrital quartz grains are extending into the diagenetic overgrowths.

Dauphiné twins visualised by the EBSD method are common in detrital quartz and quartz overgrowths. We suggest that some of the twin distributions at quartz grain edges and within quartz cement–grain contacts relate to burial compaction. This implies a mechanism of crystal plastic grain-boundary deformation in burial diagenesis, invisible by conventional petrographic tools. A combination of different techniques is suggested to reveal detailed relations of grain boundary deformation and cementation.

Acknowledgements

Parts of the analytical work have been supported by a grant from strategic programmes at NTNU. The detailed referee comments from Jeffrey Lloyd and Alvar Braathen are appreciated.

References

Aplin, A.C., Warren, E.J., Grant, S.M., Robinson, A.G., 1993. Mechanisms of quartz cementation in North Sea Reservoir sandstones: Constraints from fluid compositions. In: Horbury, A.D., Robinson, A.G. (Eds.), Diagenesis and Basin Development. American Association of Petroleum Geologists, Studies in Geology, 36, pp. 5–22.

Barber, D.J., 1985. Dislocations and microstructures. In: Wenk, H.R. (Ed.), Preferred Orientations in Deformed Metals and Rocks—An Introduction to Modern Textural Analysis. Academic Press, London.

Beard, D.C., Weyl, P.K., 1973. Influence of texture on porosity and permeability of unconsolidated sand. American Association of Petroleum Geologists Bulletin 57, 349–369.

Bjørkum, P.A., 1996. How important is pressure in causing dissolution of quartz in sandstones? Journal of Sedimentary Research 66, 147–154.

Bjørlykke, K., Aagaard, P., Dypvik, H., Hastings, D.S., Harper, A.S., 1986. Diagenesis and reservoir properties of Jurassic sandstones from the Haltenbanken area, offshore mid Norway. In: Spencer, A.M. (Ed.), Habitat of Hydrocarbons on the Norwegian Continental Shelf. Norwegian Petroleum Society, Graham & Trotman, pp. 275–286.

Bjørlykke, K., Ramm, M., Saigal, G.C., 1989. Sandstone diagenesis and porosity modification during basin evolution. Geologische Rundshau 68, 1151–1171.

Blystad, P., Brekke, H., Færseth, R.B., Larsen, B.T., Skogseid, J., Tørudbakken, B., 1995. Structural elements of the Norwegian continental shelf. Part II: The Norwegian Sea Region. Norwegian Petroleum Directorate-Bulletin 8.

Boggs Jr., S., 1992. Petrology of Sedimentary Rocks. Macmillan Publishing Company.

Brekke, H., Sjulstad, H.I., Magnus, C., Williams, R., 2001. Sedimentary environments offshore Norway—an overview. In: Martinsen, O.J., Dreyer, T. (Eds.), Sedimentary Environments Offshore Norway—Palaeozoic to Recent. Norwegian Petroleum Society Special Publication, 10, pp. 7–37.

Chester, J.S., Lenz, S.C., Chester, F.M., Lang, R.A., 2004. Mechanism of compaction of quartz sand at diagenetic conditions. Earth and Planetary Science Letters 220, 435–451.

Dalland, A., Augedahl, H.O., Bomstad, K., Ofstad, K., 1988. The post-Triassic succession of the Mid-Norwegian Shelf. In: Dalland, A., Worsley, D., Ofstad, K. (Eds.), A Lithostratigraphic Scheme for the Mesozoic and Cenozoic Succession Offshore Mid- and Northern Norway. Norwegian Petroleum Directorate Bulletin, 4, pp. 5–42.

Ehrenberg, S.N., 1990. Relationship between diagenesis and reservoir quality in sandstones of the Garn formation, Haltenbanken, Mid-Norwegian continental shelf. American Association of Petroleum Geologists Bulletin 74, 1538–1558.

Ehrenberg, S.N., 1993. Preservation of anomalously high porosity in deeply buried sandstones by grain-coating chlorite: examples from the Norwegian continental shelf. American Association of Petroleum Geologists Bulletin 77, 1260–1286.

Fisher, Q.J., Casey, M., Clennel, M.B., Knipe, R.J., 1999. Mechanical compaction of deeply buried sandstones of the North Sea. Marine and Petroleum Geology 16, 605–618.

Fjær, E., Holt, R.M., Horsrud, P., Raaen, A.M., Risnes, E., in press. Petroleum Related Rock Mechanics. Developments in Petroleum Science 33, second ed. Elsevier.

Frondel, C., 1962. Dana's System of Mineralogy: III. Silica Minerals. John Wiley and Sons, New York.

Gallagher Jr., J.J., Friedman, M., Handin, J., Sowers, G.M., 1974. Experimental studies relating to microfractures in sandstones. Tectonophysics 21, 203–248.

Giles, M.R., Indrelid, S.L., Beynon, G.V., Amthor, J., 2000. The origin of large scale quartz cementation: evidence from large data sets and coupled heat-fluid mass transport modelling. Special Publications International Association of Sedimentologists 29, 21–38.

Gjelberg, J., Dreyer, T., Høie, A., Tjelland, T., Lilleng, T., 1987. Late Jurassic to Mid-Jurassic sandbody development on the Barents and Mid-Norwegian shelf. In: Brooks, J., Glennie, K. (Eds.), Petroleum Geology of Northwest Europe. Graham & Trotman, London, pp. 1105–1129.

Gluyas, J.G., Robinson, A.G., Grant, S.M., 1993. Geochemical evidence for a temporal control on sandstone cementation. In: Horbury, A.D., Robinson, A.G. (Eds.), Diagenesis and Basin Development. American Association of Petroleum Geologists Studies in Geology, 36, pp. 23–34.

Goldstein, J.I., Newbury, D., Joy, D., Lyman, C., Echlin, P., Lifshin, E., Sawyer, L., Michael, J., 2003. Scanning Electron Microscopy and X-ray

Microanalysis. Kluwer Academic/Plenum Publishers, New York, pp, 1 CD-ROM689.

Groshong Jr., R.H., 1988. Low temperature deformation mechanisms and their interpretation. Geological Society of America Bulletin 100, 1329–1360.

Haddad, S.C., Worden, R.H., Prior, D.J., Smalley, P.C., 2006. Quartz cement in the Fountainbleau sandstone, Paris Basin, France: crystallography and implications for mechanisms of cement growth. Journal of Sedimentary Research 76, 244–256.

Hartley, N.E.W., Wilshaw, T.R., 1973. Deformation and fracture of synthetic α-quartz. Journal of Materials Sciences 8, 265–278.

Hjelen, J., Ørsund, R., Hoel, E., Runde, P., Furu, T., Nes, E., 1993. EBSP, Progress in technique and applications. Textures and Microstructures 20, 29–40.

Humphreys, F.J., 2001. Grain and subgrain characterisation by electron backscatter diffraction. Journal of Materials Science 36, 3833–3854.

Karlsen, D.A., Skeie, J.E., Backer-Owe, K., Bjørlykke, K., Olstad, R., Berge, K., Cecchi, M., Vik, E., Schaefer, R.G., 2004. Petroleum migration, faults and overpressure. Part II. Case history: The Haltenbanken Petroleum Province, offshore Norway. In: Cubitt, J.M., England, W.A., Larter, S. (Eds.), Understanding Petroleum Reservoirs: Towards an Integrated Reservoir Engineering and Geochemical Approach. Geological Society of London, Special Publications, 2347, pp. 305–372.

Knipe, R.J., 1989. Deformation mechanisms—recognition from natural tectonites. Journal of Structural Geology 11, 127–146.

Lander, R.H., Walderhaug, O., 1999. Predicting porosity through simulating sandstone compaction and quartz cementation. American Association of Petroleum Geologists Bulletin 83, 433–449.

Laughner, J.W., Cline, T.W., Newnham, R.E., Cross, L.E., 1979. Acoustic emissions from stress-induced Dauphiné twinning in quartz. Physics and Chemistry of Minerals 4, 129–137.

Lien, T., Midtbø, R.E., Martinsen, O.J., 2006. Depositional facies and reservoir quality of deep-marine sandstones in the Norwegian Sea. Norwegian Journal of Geology 86, 71–92.

Lloyd, G.E., 1987. Atomic number and crystallographic contrast images with the SEM: a review of backscattered electron techniques. Mineralogical Magazine 51, 3–19.

Lloyd, G.E., 2000. Grain boundary contact effects during faulting of quartzite: an SEM/EBSD analysis. Journal of Structural Geology 22, 1675–1679.

Makowitz, A., Milliken, K.L., 2003. Quantification of brittle deformation in burial compaction, Frio and Mount Simon Formation sandstones. Journal of Sedimentary Research 73, 1007–1021.

McBride, E.F., 1989. Quartz cement in sandstones: a review. Earth Science Reviews 26, 69–112.

Milliken, K.L., Lauback, S.E., 2000. Brittle deformation in sandstone diagenesis revealed by scanned cathodoluminescence imaging with application to characterization of fractured reservoirs. In: Pagel, M., Barbin, V., Blanc, P., Ohnenstetter, D. (Eds.), Cathodoluminescence in Geoscience. Springer, Berlin, pp. 225–243.

Moen, K., Hjelen, J., Malvik, T., 2003. Preparation of Quartz samples for EBSD analysis [Poster]. Applied Mineralogy '03, Helsinki 2003. Applied Mineralogy' 03, CD.

Morton, A.C., Grant, S., 1998. Cretaceous depositional systems in the Norwegian Sea: heavy mineral constraints. American Association of Petroleum Geologists Bulletin 82, 274–290.

Mørk, M.B.E., Johnsen, S.O., 2005. Jurassic sandstone provenance and basement erosion in the Møre margin—Froan Basin area. Norges geologiske undersøkelse Bulletin 443, 5–18.

Nord, G.L., 1994. Transformation-induced twin-boundaries in minerals. Phase Transitions 48, 107–134.

Oelkers, E.H., Bjørkum, P.A., Murphy, W.M., 1996. A petrographic and computational investigation of quartz cementation and porosity reduction in North Sea sandstones. American Journal of Science 296, 420–452.

Passchier, C.W., Trouw, R.A.J., 2005. Microtectonics. Springer, New York.

Paxton, S.T., Szabo, J.O., Ajdukiewicz, J.M., Klimentidis, R.E., 2002. Construction of an intergranular volume compaction curve for evaluating and predicting compaction and porosity loss in rigid-grain sandstone reservoirs. American Association of Petroleum Geologists Bulletin 86, 2047–2067.

Pettersen, T., Heiberg, G., Hjelen, J., 1998. Measurements of spatial resolution of EBSP in the SEM as a function of atomic number and high voltage. The 14th International Congress on Electron Microscopy, Cancun, Mexico, 1998.

Pettijohn, F.J., Potter, P.E., Siever, R., 1972. Sand and Sandstone. Springer, New York.

Piazolo, S., Prior, D.J., Holness, M.D., 2005. The use of combined cathodoluminescence and EBSD analysis: a case study investigating grain boundary migration mechanisms in quartz. Journal of Microscopy 217, 152–161.

Prior, D.J., Boyle, A.P., Brenker, F., Cheadle, M.C., Day, A., Lopez, G., Peruzzi, L., Potts, G.J., Reddy, S., Spiess, R., Timms, N.E., Trimby, P., Wheeler, J., Zetterström, L., 1999. The application of electron backscatter diffraction and orientation contrast imaging in the SEM to textural problems in rocks. American Mineralogist 84, 1741–1759.

Putnis, A., 1992. Introduction to Mineral Sciences. Cambridge University Press, Cambridge.

Renard, F., Ortoleva, P., 1997. Water film at grain-grain contacts: Debye-Huckel osmoic model of stress, salinity and mineralogy dependence. Geochimica et Cosmochimica Acta 61, 1963–1970.

Renard, F., Brosse, É., Gratier, J.P., 2000. The different processes involved in the mechanism of pressure solution in quartz-rich rocks and their interactions. Special Publications International Association of Sedimentologists 29, 67–78.

Schmidt, N.H., Olesen, N.O., 1989. Computer-aided determination of crystal lattice orientation from electron channeling patterns in the SEM. Canadian Mineralogist 27, 15–22.

Schutjens, P.M.T.M., 1991. Experimental compaction of quartz sand at low effective stress and temperature conditions. Journal of the Geological Society of London 148, 527–539.

Schwartz, A.J., Kumar, M., Adams, B.L., 2000. Electron Backscatter Diffraction in Materials Science. Kluwer Academic/Plenum Publishers, New York.

Shanmugam, G., Lehtonen, L.R., Straume, T., Syvertsen, S.E., Hodgkinson, R.J., Skibeli, M., 1994. Slump and debris-flow dominated upper slope facies in the Cretaceous of the Norwegian and Northern North Seas (61–67°N): Implications for sand distribution. American Association of Petroleum Geologists Bulletin 78, 910–937.

Sippel, R.F., 1968. Sandstone petrology, evidence from luminescence petrography. Journal of Sedimentary Petrology 38, 530–554.

Spencer, A.M., Birkeland, Ø., Koch, J.-O., 1993. Petroleum geology of the proven hydrocarbon basins, offshore Norway. First Break 11, 161–176.

Storvoll, V., Bjørlykke, K., Karlsen, D., Saigal, G., 2002. Porosity preservation in reservoir sandstones due to grain-coating illite: a study of the Jurassic Garn Formation from the Kristin and Lavrans fields, offshore Mid-Norway. Marine and Petroleum Geology 19, 767–782.

Terry, M.P., Heidelbach, F., 2006. Deformation enhanced metamorphic reactions and the rheology of high-pressure shear zones. In: Journal of Metamorphic Geology, 24. Western Gneiss region, Norway. 3–18.

Thomson, A., 1959. Pressure solution and porosity. In: Ireland, H.A. (Ed.), Silica in Sediments. Society for Sedimentary Geology Special publication, 7, pp. 92–111.

Tullis, J., 1970. Preferred orientation in rocks produced by Dauphiné twinning. Science 168, 1342–1344.

Vagle, G.B., Hurst, A., Dypvik, H., 1994. Origin of quartz cements in some sandstones from the Jurassic of the Inner Moray Firth (UK). Sedimentology 41, 363–377.

Valcke, S.L.A., Casey, M., Lloyd, G.E., Kendall, J.-M., Fisher, Q.J., 2006. Lattice preferred orientation and seismic anisotropy in sedimentary rocks. Geophysical Journal International 166, 652–666.

van Daalen, M., Heilbronner, R., Kunze, K., 1999. Orientation analysis of localized shear deformation in quartz fibres at the brittle-ductile transition. Tectonophysics 303, 83–107.

Vernon, R.H., 2004. A Practical Guide to Rock Microstructure. Cambridge University Press.

Vernon, R.H., 1981. Optical microstructure of partly recrystallized calcite in some naturally deformed marbles. Tectonophysics 78, 601–612.

Walderhaug, O., 1994. Temperatures of quartz cementation in Jurassic sandstones from the Norwegian continental shelf—Evidence from fluid inclusions. Journal of Sedimentary Research 64, 311–323.

Walderhaug, O., 1996. Kinetic modeling of quartz cementation and porosity loss in deeply buried sandstone reservoirs. American Association of Petroleum Geologists Bulletin 80, 731–745.

Walderhaug, O., Bjørkum, P.A., 2003. The effect of stylolite spacing on quartz cementation in the Lower Jurassic Stø Formation, southern Barents Sea. Journal of Sedimentary Research 73, 146–156.

Wenk, H.-R., Lonardelli, I., Vogel, S.C., Tullis, J., 2005. Dauphiné twinning as evidence for an impact origin of preferred orientation in quartzite: an example from Vredefort, South Africa. Geological Society of America Bulletin 33, 273–276.

Wenk, H.-R., Rybacki, E., Dresen, G., Lonardelli, I., Barton, N., Franz, H., Gonzalez, G., 2006. Dauphiné twinning and texture memory in polycrystalline quartz. Part 1: Experimental deformation of novaculite. Physics and Chemistry of Minerals 33, 667–676.

White, S.H., 1977. Geological significance of recovery and recrystallisation processes in quartz. Tectonophysics 39, 143–170.

Worden, R.H., Burley, S.D., 2003. Sandstone diagenesis: The evolution of sand to stone. In: Burley, S.D., Worden, R.H. (Eds.), Sandstone Diagenesis. Recent and Ancient. Reprint Series 4 of the International Association of Sedimentologists. Blackwell Publishing, pp. 3–44.

Wright, S., 2005. A Collection of OIM applications. In: Wright, S. (Ed.). Edax TSL, p. 106.